



Enabling fast charging – Battery thermal considerations



Matthew Keyser^{a,*}, Ahmad Pesaran^a, Qibo Li^a, Shriram Santhanagopalan^a, Kandler Smith^a, Eric Wood^a, Shabbir Ahmed^b, Ira Bloom^b, Eric Dufek^c, Matthew Shirk^c, Andrew Meintz^a, Cory Kreuzer^a, Christopher Michelbacher^c, Andrew Burnham^b, Thomas Stephens^b, James Francfort^c, Barney Carlson^c, Jiucai Zhang^a, Ram Vijayagopal^b, Keith Hardy^b, Fernando Dias^c, Manish Mohanpurkar^c, Don Scofield^c, Andrew N. Jansen^b, Tanvir Tanim^c, Anthony Markel^a

^a National Renewable Energy Laboratory, 15013 Denver West Parkway, Golden, CO 80401, USA

^b Argonne National Laboratory, 9700 South Cass Avenue, Argonne, IL 60439, USA

^c Idaho National Laboratory, 2525 N. Fremont, Idaho Falls, ID 83415, USA

HIGHLIGHTS

- Aggressive thermal management will be required during extreme fast charging.
- Present high energy density cells will need to increase their charge efficiency.
- Cell design will have an impact on the temperature variation within the cell.
- Battery interconnects will need to be robust and may require a redesign.

ARTICLE INFO

Article history:

Received 21 April 2017

Received in revised form

19 June 2017

Accepted 3 July 2017

Keywords:

Lithium-ion battery

Extreme fast charging

Battery thermal efficiency

Battery thermal management

Cell thermal design

Heat generation

ABSTRACT

Battery thermal barriers are reviewed with regards to extreme fast charging. Present-day thermal management systems for battery electric vehicles are inadequate in limiting the maximum temperature rise of the battery during extreme fast charging. If the battery thermal management system is not designed correctly, the temperature of the cells could reach abuse temperatures and potentially send the cells into thermal runaway. Furthermore, the cell and battery interconnect design needs to be improved to meet the lifetime expectations of the consumer. Each of these aspects is explored and addressed as well as outlining where the heat is generated in a cell, the efficiencies of power and energy cells, and what type of battery thermal management solutions are available in today's market. Thermal management is not a limiting condition with regard to extreme fast charging, but many factors need to be addressed especially for future high specific energy density cells to meet U.S. Department of Energy cost and volume goals.

© 2017 Elsevier B.V. All rights reserved.

1. Introduction

Extreme fast charging (XFC) allows a 200-mile battery pack in a battery electric vehicle (BEV) to be recharged as fast as a conventional vehicle can be refueled. However, XFC will require research and development to address the significant impacts of XFC on the infrastructure, corridor planning, cost of vehicle ownership, battery

chemistry, and deployment economics. While XFC promises to help the adoption of BEVs and curb greenhouse gas emissions and America's need for imported oil, designing high-performance, cost-effective, safe, and affordable energy-storage systems for these BEVs can present challenges, especially in the critical area of battery thermal control. As manufacturers strive to make batteries more compact and powerful, knowing how and where heat is generated becomes even more essential to the design of effective battery thermal management systems (BTMSs).

Enabling XFC requires understanding and controlling the temperature of battery systems. The chemistries of advanced energy-

* Corresponding author.

E-mail address: Matthew.Keyser@nrel.gov (M. Keyser).

storage devices, such as lithium-based batteries, are very sensitive to operating temperature. High temperatures degrade batteries faster while low temperatures decrease their power and capacity, affecting vehicle range, performance, and cost. Understanding heat generation in battery systems—from the individual cells within a module to the interconnects between the cells and across the entire battery system—is imperative for designing effective BTMSs and battery packs.

The 2022 U.S. Department of Energy's (DOE's) battery goals of 350 Wh kg⁻¹, 1000 Wh L⁻¹, and \$125 kWh⁻¹ [1] require battery packs that have higher energy densities, resulting in a very compact system. To meet the specific energy goal, the electrode thickness of the battery will need to increase while decreasing the thickness of the current collectors. Furthermore, the amount of electrochemically inactive material, such as binders, will need to decrease. All of these factors will have a deleterious effect on the thermal performance of the cell. Furthermore, many of the advanced chemistries being developed to attain these goals, such as silicon and lithium metal anodes along with high-energy cathodes, have heretofore suffered from low efficiencies at low to moderate charge and discharge rates. Even if the energy efficiency of the next generation of batteries increases, more heat is being generated per unit volume with a smaller heat transfer area because of the compactness of these batteries. Thus, combining the heat transfer limitations associated with advanced chemistries with XFC will challenge the battery designers to keep the battery temperatures in the “Goldilocks” zone that prevents acceleration of the aging mechanisms within the battery while limiting the cycle life cost.

In 2012, Nissan had to address problems with the battery of its Leaf fully electric vehicle (EV), which was losing capacity in the hot Arizona climate. Many experts in the field attributed this issue to inadequate battery thermal management. Using XFC to enable the penetration of EVs but ignoring their thermal design will negatively affect lifespan, safety, and cost, ultimately resulting in negative consumer perception and reduced marketability.

2. Review of the heat produced in a battery cell and pack

2.1. Battery heat generation

Lithium-ion batteries have very good coulombic cycling efficiencies, as high as 99.5%. The small drop in efficiency is often traced back to a mismatch of properties among the different components (e.g., differences in the rate of transport of electrons versus the ions) and manifests itself in the form of heat. Heat generated within the battery is usually classified into reversible entropic heats and irreversible losses due to low conversion rates for the chemical reactions, or poor transport properties resulting in some polarization losses. Some of these losses are minimized by suitable design changes to the cells. One example is matching the porosity of the electrodes to that of the separator membrane. Mitigation of other types of losses may involve changes to the chemistry of the electrode or the composition of the electrolyte. Tracing back the efficiency losses at the cell level to the relevant contribution from each source will enable battery manufacturers to evaluate tradeoffs between the efficiency improvements and cost of redesigning the cells.

- **Heat Generation from Joule Heating:** Joule heating losses within a cell arise primarily from poor electronic conductivities within the solid phase of the cell, low electrolyte conductivities, contact resistances at the junctions between cell components, or formation of a resistive film on the electrode surface from electrolyte decomposition reactions. Ohmic losses are a function of

the C-rate, size, and age of the cells. Ohmic losses can constitute up to 50% of the heat budget [2].

- **Heat Generation from Electrode Reactions:** Electrochemical reactions taking place within the cells involve transfer of charge at the interface between the electrodes and the electrolyte when the circuit is closed. The mobilities of the bulkier ions are about seven orders of magnitude smaller than those of the electrons, and the difference in the electrochemical potentials for lithium ions within the host lattice at the electrode and within the electrolyte governs the rate of charge transfer. Transfer of charge across the energy barrier at the interface results in loss of a part of the kinetic energy associated with these reactions. Heat losses due to the charge transfer process are measured as the difference in free energies across the two sides of the interface. Whereas sluggish kinetics have been known to limit efficiencies in some chemistries (e.g., in some phosphate-based cathodes), activation barriers usually contribute to 30%–40% of the heat losses under practical operating cases [2].
- **Entropic Heat Generation:** Insertion and de-insertion of lithium ions in and out of the electrodes result in entropic changes within the electrodes. Ideally, such changes are reversible under very slow rates of charge and discharge; however, from a practical perspective, there is some energy loss associated with these phenomena. Usually, the entropic losses in an electrode take place at well-defined voltage windows. Such entropic losses constitute the reversible portion of heat generation. Whereas these changes can be as low as 5%–10% of the total heat budget [2], changes to the entropy of the host lattice are often accompanied by additional limitations such as changes to mechanical properties or phase changes, which complicate the analysis of the impact of such losses on the durability of the cell.

2.2. Heat generation of high energy density cells

Fig. 1 shows the heat efficiency of two cells—energy and power—tested in a large volume isothermal calorimeter. The graph shows a full discharge from 100% to 0% state of charge. The data are limited due to the discharge limitations for the energy cell under test. The maximum continuous discharge rate as specified by the manufacturer was 2C. The power cell in Fig. 1 has a capacity of 6 Ah whereas the energy cell has a capacity of 20 Ah. The thermal heat efficiency is representative of most energy and power cells tested in the calorimeter. Due to the thickness of the coatings (cathode and

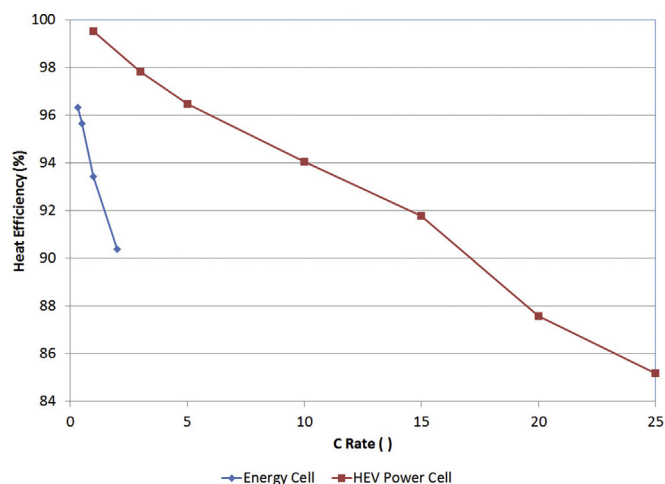


Fig. 1. Discharge efficiency of an energy cell and a power cell at 30 °C.

anode) and the thickness of the current collectors, the efficiency of the energy cells is well below that of the power cell – both cells are of the same chemistry, NMC/graphite. As a rule of thumb, the charge efficiency for graphitic cells is typically 2%–8% less than the discharge efficiency. In the end, the state-of-the-art energy cells have efficiencies that will limit them from being used in XFC scenarios.

To attain DOE's goals of 350 Wh kg^{-1} and $\$125 \text{ kWh}^{-1}$, new cathodes and anodes need to be investigated. On the cathode side, nickel or manganese rich nickel-manganese-cobalt (NMC) has the potential to help with the energy density of the cells; however, cathodes and anodes both have issues with dissolution of the excess metal used in their chemistry. We are also investigating both silicon and lithium anodes to meet the specific energy density goals. Silicon has expansion/contraction issues when cycling as well as irreversible capacity loss after the first cycle, and a pure lithium anode comes with many safety challenges. Both advanced cathodes and anodes were tested in an isothermal calorimeter. Their discharge efficiencies as a function of C-rate are shown in Fig. 2. The advanced NMC cathode with a graphitic anode was tested at 30°C and has a capacity of approximately 20 Ah. The discharge efficiency for this cell at a 2C rate is about 81%. Fig. 2 also shows a lithium anode cell with a solid electrolyte. The solid electrolyte helps to address safety concerns but has poor ionic diffusivity at room temperature, so the test was run at an ambient temperature of 80°C . The efficiency for the lithium anode under a constant current discharge approaches 94%, but only for a C/2 discharge rate. In comparison, present high-power lithium-ion cells used in EVs have a discharge efficiency of about 99% under a C/2 discharge and at an ambient temperature of 30°C . The solid electrolyte limits the rate and temperature at which the cell can be used, which limits their present use in EVs. Improvements to both the cathode and anode need to be made to meet the DOE's energy and cost goals, and the efficiency of these advanced cells will also need to be improved to meet the demands of XFC.

2.3. Cell temperature study under XFC

To better understand the heat transfer limitations with regards to extreme fast charging, a lumped heat transfer analysis and a 3-D simulation for a standard lithium ion cell were performed. The specification and heat transfer conditions of battery pack are shown in Table 1 and Table 2, respectively.

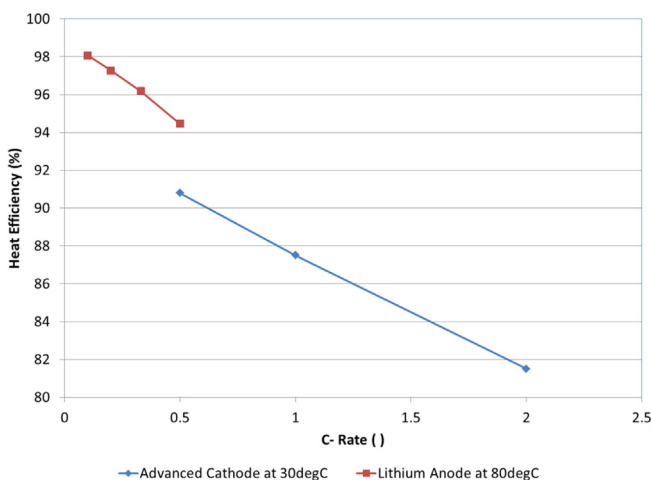


Fig. 2. Discharge efficiency of a cell with an advanced NMC cathode and a cell with a lithium anode.

Table 1
Battery pack specification.

Performance Characteristics	Typical	Unit
Maximum Range Provided	200	Miles
Energy Used Mile ⁻¹	0.33	kWh mile ⁻¹
Pack Energy	66	kWh
Charger Power	350	kW

Table 2
Battery pack heat transfer conditions.

	Lower Limit	Upper Limit
Battery Regen/Charge Efficiency (%)	70	90
Pack Heat Generation (kW)	116	39
Heat Transfer Coefficient ($\text{W m}^{-2} \text{K}^{-1}$)	10	100
Cooling Provided (kW)	2	15
Energy Density (Wh kg^{-1})	175	300

In this study, we modeled a single cell within the battery pack. The specification and geometry of battery cell are shown in Table 3.

To understand the effects of heat transfer conditions and energy density of the battery on temperature of single battery cell, four cases were selected for this study as shown in Table 4. At the beginning of each simulation, the heat transfer coefficients specified in Table 4 are the limiting condition for heat transfer. As the cell heats and the available cooling power increases, the limiting condition is the total thermal power removed per cell.

The 3-D simulation was performed using the commercially available ANSYS/Fluent software. For the 3-D simulation, the heat transfer coefficient and cooling are being provided to the large surfaces of the cell, not to the terminals or edges; all other surfaces of the battery cell are assumed to be under adiabatic conditions. The ambient temperature and initial cell temperature were assumed to be 23°C .

The battery cell was divided into 31 sets of layers. Each layer includes the aluminum current collector, cathode, separator, anode, and copper current collector. The properties for these cell components are shown in Table 5.

Fig. 3 shows the cell temperature rise for the four individual cases during the 350-kW XFC. The figure shows that Cases 2 and 4 have the lowest temperature rise, and the temperature rise for Cases 1 and 3 are approaching abuse levels—greater than 200°C after 750 s. For Cases 1 and 3, the charge efficiency of the cell is 70% (typical charge efficiency for high energy density cells), and the thermal management system is only providing 2 kW of cooling to the pack. When comparing Cases 2 and 4, the cell energy density for Case 4 is the lowest, which leads to the maximum number cells needed to provide a 200-mile range for the EV. Thus, the heat generation per cell is much lower for Case 4 with the largest available surface area to remove the heat: more cells leads to more surface area. It should be noted that both Cases 2 and 4 have the same total pack cooling power, 15 kW, which is substantially oversized as compared to the cooling systems for most EVs presently on the market. In summary, when heat transfer conditions for the battery packs are the same, the cell with the lower energy density yields an overall lower cell temperature.

This simplified study yields a few interesting conclusions. With

Table 3
Cell geometry and mass.

	Typical	Unit
Mass of Single Cell	0.78	kg
Dimensions of Single Cell (T × W × H)	$7.9 \times 225 \times 190.5$	mm

Table 4

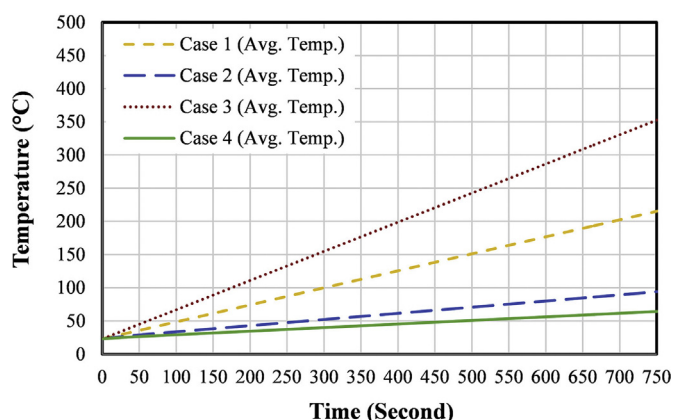
Case conditions under a constant 350-kW charge.

Case 1			Case 2		
Energy Density	175	Wh kg ⁻¹	Energy Density	300	Wh kg ⁻¹
Number of Cells	484	cells	Number of Cells	282	cells
Cell Efficiency	70	%	Cell Efficiency	90	%
Pack Heat Removed	2	kW	Pack Heat Removed	15	kW
Heat Generation per Cell	239.9	W	Heat Generation per Cell	138.3	W
Cooling Provided per Cell	4.14	W	Cooling Provided per Cell	53.2	W
Heat Transfer Coefficient	10	W m ⁻² K ⁻¹	Heat Transfer Coefficient	100	W m ⁻² K ⁻¹
Case 3			Case 4		
Energy Density	300	Wh kg ⁻¹	Energy Density	175	Wh kg ⁻¹
Number of Cells	282	cells	Number of Cells	484	cells
Cell Efficiency	70	%	Cell Efficiency	90	%
Pack Heat Removed	2	kW	Pack Heat Removed	15	kW
Heat Generation per Cell	411.3	W	Heat Generation per Cell	80.7	W
Cooling Provided per Cell	7.1	W	Cooling Provided per Cell	31	W
Heat Transfer Coefficient	10	W m ⁻² K ⁻¹	Heat Transfer Coefficient	100	W m ⁻² K ⁻¹

Table 5

Properties of battery cell with multiple layers.

Properties	Thickness (μm)	C _p (J kg ⁻¹ K ⁻¹)	Density (kg m ⁻³)	K-cross plane (W m ⁻¹ K ⁻¹)	K-in plane (W m ⁻¹ K ⁻¹)
Al current collector	20	889	2700	235	235
Cathode	43	973	3611	1.03	19.15
Separator	22	2057	1107	0.31	0.31
Anode	46	1111	1907	2.36	28.18
Cu current collector	14	378	8880	400	400

**Fig. 3.** Average temperature rise of a single battery cell for Cases 1, 2, 3, and 4.

an oversized BTMS of 15 kW and low energy density cells (power cells), it is possible to design a system that may be able to charge at 350 kW without hitting the DOE's maximum operating temperature goal of 52 °C. From the Case 4 scenario above, the end temperature of the cell would be around 56 °C from a starting temperature of 23 °C after charging for 600 s or at a 6C rate. However, when using a cell with an energy density of 175 Wh kg⁻¹ as in the Case 4 scenario, the penalty to the vehicle would be increased mass, volume, and cost. The typical power cell has thinner material coatings on the cathode and anode as well as thicker aluminum and copper current collectors. All of these contribute to higher power cells but also increase the battery pack cost due to the loss of active material. The typical lithium ion power cell costs between \$400–\$600 kWh⁻¹. In the end, we can come close to meeting the thermal targets of charging at 350 kW by using power cells but with a cost, volume, and mass penalty. However, we need to take other factors into consideration before making such a sweeping generalization.

2.4. Battery temperature variation and design

The 3-D study described above assumes that all the heat generation within the cell is spread equally across the volume of the cell, which is obviously an over-simplification. Furthermore, Section 2.3 assessed how the average temperature of the cell varies as a function of energy density and heat transfer characteristics but the temperature variance within the cell also needs to be evaluated, especially for XFC conditions. NREL previously performed an empirical study [3] on varying the length scales and tab designs for a lithium cell to determine the temperature effects of a fast rate discharge. The models used for the discharge study were modified here to simulate a fast rate (6C) charge. Fig. 4 summarizes the four different cell designs investigated during the study.

In the fast charge study, the cell design was varied to assess the volumetric temperature variation and these results are presented in Fig. 5. In Fig. 5, temperature contours at nine cross-sectioned surfaces of each cell are presented to show details of the spatial temperature imbalance at the end of charge. The average charge efficiency for each of the cell designs was calculated to be approximately 90%, which is the typical efficiency of a power cell under a high rate charge. The results clearly show how the tab and cell design affects the temperature distribution within the cell but also how the interior cell temperature varies across its volume. The most thermally uniform cell is the counter tab design, a 2.9 °C difference across the cell, whereas the least thermally uniform is the small tab design, a temperature difference of 4.4 °C. The maximum temperature of the cell needs to be limited during XFC, but the temperature difference across the cell will also impact the cell cost and life.

The cell thermal contour study was performed using high-power cells where the battery material and design were optimized for today's hybrid electric vehicles. As a counter point, Fig. 6 shows the thermal image of a high-energy NMC/graphite advanced chemistry 18-Ah cell that was designed exclusively for EV applications. The figure contains a thermal image of the cell at the end of

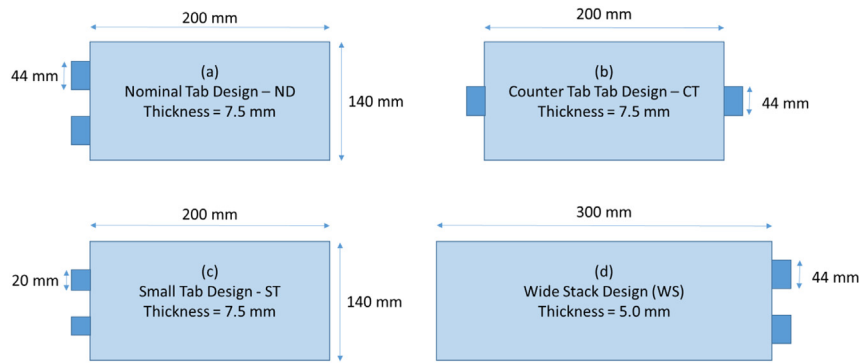


Fig. 4. Schematic description of the 20-Ah stacked pouch cell designs.

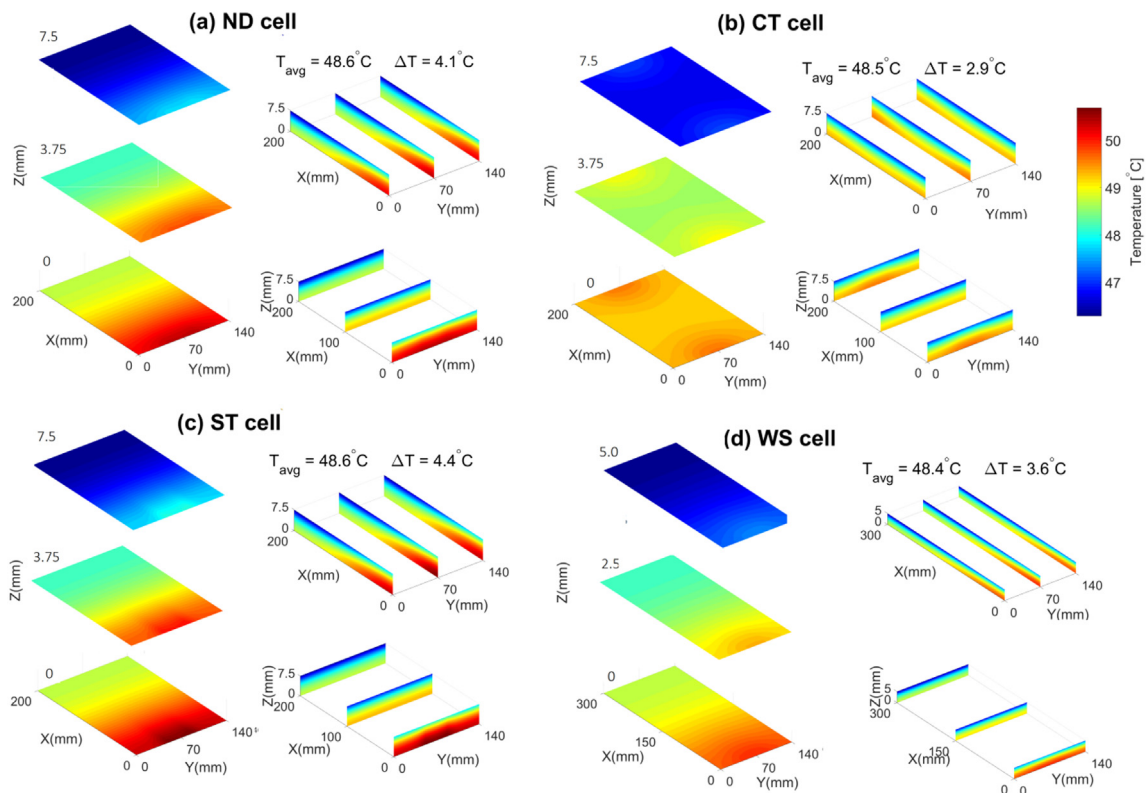


Fig. 5. Contours of temperature at nine cross-sectioned surfaces in cell composite volume at the end of 6C constant current charge: (a) ND cell, (b) CT cell, (c) ST cell, (d) WS cell. (Dimensions in Z direction of the contour surfaces are exaggerated for a clearer view of quantity variation in Z direction.)

a 2C constant current discharge as well as a plot showing horizontal contour lines across the face of the cell – L01, L02, L03, and L04. The cell had an initial temperature of 23 °C. Fig. 6 shows a hot spot in the upper left corner of the thermal image of the cell as well as a wide spread in temperature across the face of the cell from top to bottom and left to right – the active area surface temperature varies by about 6 °C. When the cell temperature is non-uniform and inconsistent, areas within the cell age at different rates, leading to poor cycle life: areas of the cell that are higher in temperature are more efficient and therefore age faster due to higher power loads [4]. It should be noted that the high-energy NMC cells are prone to gassing during cycling, and further research and development will be necessary to incorporate these cells in BEV and XFC applications.

To enable XFC, cell designs may need to be modified to minimize the time constant for the heat generated within the cell to get to the

primary cooling plate, liquid, etc., during XFC. If the time constant is large, the heat will not be able to get from the cell interior to the cooling system. Methods to adjust the cooling path may include:

- Increasing the amount of carbon black or other conductive material in the cathode and anode [5].
- Increasing the thickness of the current collectors.
- Incorporating low temperature phase change material within the cell to absorb heat where it is generated. However, it may not be feasible to modify the cell with an electrochemically inert material.
- Continuous current collectors have a more optimal heat conductive path but would limit the cell design options.

All of the above suggestions will have an impact on the energy

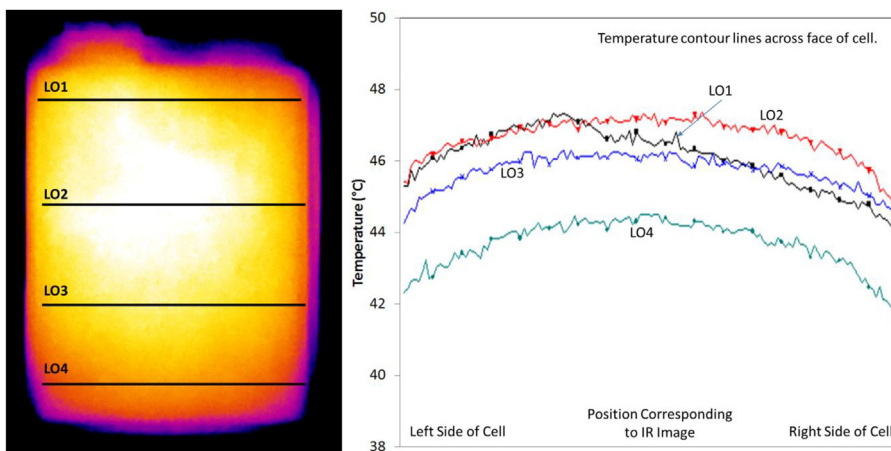


Fig. 6. Thermal image and temperature plot of a high-energy NMC/graphite cell at the end of a 2C constant current discharge from 100% to 0% state of charge.

density of the battery and will therefore affect the range of the vehicle. However, they may be necessary to keep the battery cool during XFC.

2.5. Module interconnect design

To understand the heat generation in a module due to the battery interconnects, the heat generation of a lithium-iron-phosphate/graphite cell was measured individually and when incorporated into a 10-cell module. The module was designed for a hybrid electric vehicle application, and the cells were considered to be power cells with a power-to-energy ratio of greater than 10 – the power-to-energy ratio is defined as the maximum battery power for a known period of time divided by the overall energy stored in the battery. Fig. 7 shows a comparison of the heat generation of a single lithium-iron-phosphate/graphite cell and the heat generation per cell for the module at various discharge currents – the difference in heat rate/cell is due to the interconnects between the cells in the module. The root mean square current for the relevant HEV application was calculated to be approximately 35 A. At this current, the heat generation normalized per cell in the module is about 22% greater than for an individual cell. Thus, even with a design optimized for high power/current, the interconnects can contribute a substantial amount of heat above and beyond the cells. For XFC applications, the heat contributed by the interconnects will need to be considered in order to mitigate potential safety

concerns.

3. Thermal management system

3.1. Battery thermal management design

During our previous 3-D temperature study in Section 3.2, we considered two BTMSs with cooling powers of 2 kW and 15 kW. The 3-D study showed that the cooling power during XFC will need to be increased beyond today’s BTMSs for BEVs, perhaps to levels greater than 15 kW, to limit the temperature rise of the cells within the pack. In the end, the BTMS ensures that the battery pack can deliver the specified load within the temperature constraints set by battery performance and life requirements across a wide range of operating conditions for the battery pack. The temperature distribution within a battery module is usually controlled tightly and is often as low as 2 °C. There are additional specifications on weight, volume, cost, energy budget, and reliability that are closely tied to the application. There are different classifications of thermal management techniques for battery packs based upon the working fluid (an air-cooled versus a liquid-cooled system) or functionality (an active cooling system with a heating or cooling source versus a passive system). A BTMS for an XFC system should carefully consider the tradeoffs between the energy budget for thermal management and the heat loads under fast charge, since an XFC system will have very different heat loads compared to conventional battery packs. Design of an optimal BTMS is often a tradeoff among the following constraints [6]:

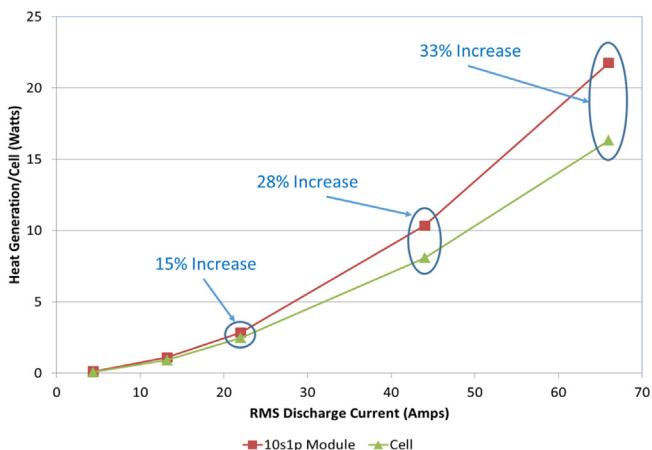


Fig. 7. Heat generation normalized on a cell basis for a single cell and a 10-cell lithium-iron-phosphate module.

- The BTMS should balance the desired thermal performance for the modules and packs under various operating conditions (e.g., specifications on the average temperature for the battery pack, minimum or maximum temperatures) with constraints on size or weight of the BTMS.
- Interfaces between the cells, as well as those between the battery and the rest of the vehicle, are important, but often overlooked aspects of thermal management.
- Safety requirements (e.g., structural specifications to sustain pressure drop for a given flow rate of the coolant) for battery packs are often different from those for other passive components within the vehicle.

3.2. Battery thermal management strategies

Today’s BTMSs typically use air, liquid, or refrigerant cooling to

manage the temperature of the cells. The air-cooling technique circulates ambient or actively cooled air through the battery pack, and the heat is rejected to the surroundings, which requires large surface areas to extract the heat. Air is typically the least expensive thermal management option, but due to its low thermal conductivity and heat capacity, it requires large flow channels and high fan power. The high fan power may also irritate some drivers due to the noise.

Liquid cooling is the preferred thermal management strategy for most BEV systems on the market today. It typically involves a combination of ethylene glycol and water as the working fluid due to the low cost. Liquid cooling systems benefit from high heat capacity and thermal conductivity as compared to air systems. However, the liquid flow channels are typically more complex and require an extensive number of connections leading to a higher potential for failure. If the liquid cooling system were to fail, then there is the potential that the liquid could short out adjacent cells within the battery pack which could lead to thermal runaway. To address this concern, a dielectric coolant could be utilized instead of an ethylene glycol/water mixture, but at a significant cost penalty. Also, dielectric fluids tend to lose their ability to insulate over time, which may require costly regular maintenance or a filtration system.

The third option is to actively cool the batteries using a vapor compression system. The typical design shunts heat from the cells in the battery pack to the evaporator of the vapor compression system using a thin metal plate. The evaporator consists of a flat plate through which the refrigerant circulates in channels or tubes. This system is more complex and with a higher initial cost and it also has reliability issues—the refrigerant will have to be contained within a hermitically sealed system for the life of the battery pack. One net positive of the system is that the evaporator plate can be cooled to sub-ambient temperatures, allowing for more thermal power to be dissipated due to the higher temperature difference between the battery cells and the cold plate. However, since the refrigerant is not in direct contact with the cells, the temperature difference across the surface of the cell may be increased.

3.3. Cooling fluid provided at direct current fast charging station

If XFC is to be utilized in vehicles, new cooling strategies may need to be developed such as jet impingement, submersion of the battery pack in a dielectric coolant, or perhaps incorporating phase change material as a buffer for XFC. External cooling provided to the vehicle at the direct current fast charging (DCFC) station should also be considered. However, what type of standardized cooling should be provided by the charging station? If chilled air is provided at the charging station, the cooling power would be limited, as indicated above, by the low heat capacity of air. The air volume required for the needed cooling power would be extremely high, limiting the use of most internal heat exchangers presently used in today's EVs. Active cooling in the form of vapor compression—i.e., providing a low-pressure refrigerant to the vehicle and integrated with the battery heat exchangers—will not be feasible. The potential for release of refrigerant would be a difficult to approve/handle from an environmental health perspective. The only feasible option would be to provide chilled water/coolant to the vehicle. If the onboard system has a different type of cooling strategy, would that mean that two heat exchanger systems are required? What would be the temperature of the cooling liquid? Would this only exacerbate the cell temperature imbalance and affect the cycle life cost of the battery. In summary, there are many thermal management questions that need to be answered before XFC will be a reality.

4. Temperature effect on battery lifetime and capacity

4.1. Temperature effect on life of battery

Lithium-ion battery life also varies greatly with cell temperature, maximum and minimum SOC, all of which are impacted by XFC. Charging C-rate is also a factor in aging; however, in test data that exists to date, it is difficult to decouple the impact of charging C-rate from coupled factors of elevated cell temperature and accelerated frequency of charge/discharge cycles per day. It would be possible to design experiments that decouple each of these factors. Different cell chemistries and power-to-energy ratio designs would respond differently to these factors.

Previous work at the National Renewable Energy Laboratory [7–9] has developed aging models of lithium-ion cells that consider the impact of temperature and charge/discharge cycle on battery life. The dominant factor, temperature, is well captured by the models. Fig. 8 shows the influence of cell yearly average temperature on battery life. Lifetime roughly doubles for each 13 °C reduction in average battery temperature. While average temperature dominates calendar life, minimum and maximum temperature extrema will also influence lifetime. It should also be noted that the critical point in the curve at approximately 80% DOD delineates the transition between calendar and cycle aging effects—below approximately 80%, the calendar ageing effects dominate whereas above 80%, the cycle ageing effects dominate [10].

Another issue related to battery temperature and lifetime is cell-to-cell capacity imbalance growth. Passive electrical cell balancing is the norm in today's BEVs due to the lower cost of those electrical controls compared to active cell balancing. With a passive balancing system, the overall battery pack's capacity is limited by the weakest cell in the series string of cells. Cells age differently, both due to manufacturing non-uniformity and cell-to-cell temperature differences across a multi-cell pack. Large packs with cells spread across the vehicle platform will experience relatively large cell-to-cell temperature differences. Depending on the thermal management design, fast charging may exacerbate cell-to-cell temperature imbalance and drive weak cells in hot locations of the pack to premature end of life. This factor remains to be quantified for XFC.

4.2. Effect of 50-kW DCFC on battery life and capacity

Although the effects of XFC have not yet been studied by the

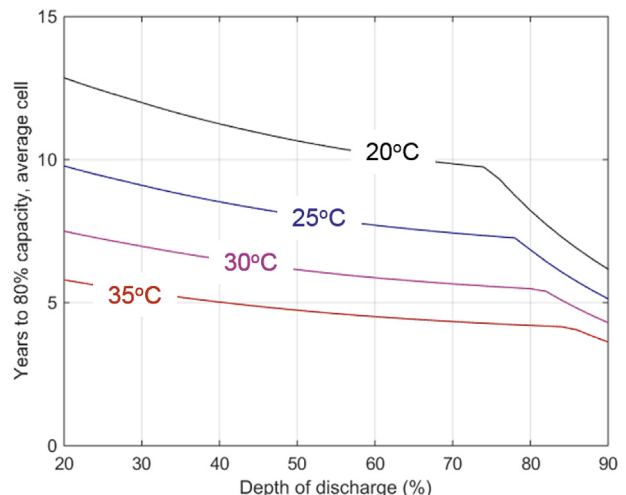


Fig. 8. Capacity fade of a NMC/Gr. cell at different average temperatures [10].

authors, the Battery Lifetime Analysis and Simulation Tool (BLAST) [11] has been used to investigate the impact of 50-kW DCFC on simulated battery degradation. The analysis also reviewed the effects of three different BTMSs (passive, active, and active with standby cooling) in two climates (Seattle, Washington (cool/wet), and Phoenix, Arizona (hot/dry)) using a simulated single-cell battery model of a nickel-cobalt-aluminum cathode and graphite anode with a power-to-energy ratio of 6.1. The study showed that the vehicles with the most extreme travel history and the largest time-averaged battery temperature had a time-averaged battery temperature increase of 2°C–3°C in the presence of a passive BTMS. Where an active BTMS is present, this effect is largely unnoticeable. As shown in Table 6, there is little impact from 50-kW DCFC on capacity loss in either Seattle or Phoenix; however, the BTMS has a significant impact on capacity in Phoenix. Past studies [12] have shown that BEV battery life is often dependent on calendar fade mechanisms rather than cycling fade mechanisms; thus, the time-averaged battery temperatures directly relate to battery capacity loss.

While the nearly negligible impact of 50-kW DCFC use on battery capacity fade may be surprising to some, it is important to point out that most drivers will use DCFCs quite sparingly. Most drivers use a DCFC less than once per month, and when DCFCs are used, they typically increase the charge of the battery by less than 60%. Further, recent tests where DCFCs are used twice per day to charge Nissan LEAFs driving in Phoenix [13] have shown that the difference in capacity loss is less than 3% due to fast charger use (as compared to an otherwise identical case using Level 2 charging) after 50,000 miles of driving. Thus, the results employing more realistic, less aggressive fast charging habits are to be expected. However, it is possible that alternative battery chemistries outside of this study could sustain considerable losses in capacity or increases in resistance due to such low frequency DCFC use (e.g., via particle fracture). Clearly, it would not be advisable to recommend fast charging such chemistries, and thus analysis of such cases is not addressed herein.

Where the effect of DCFC use is most noticeable is in the maximum achieved battery temperature. As shown in Table 7, comparison of cases with and without DCFC availability shows that maximum battery temperatures are ~15 °C higher for the median driver when fast charging is employed with a passive BTMS. In the presence of fast charging, our simulated maximum battery temperatures regularly exceed 45 °C in Seattle and 60 °C in Phoenix, so high that they could pose a safety risk if charging and/or driving are not impeded by onboard vehicle control systems. The addition of active battery cooling, however, can significantly moderate maximum battery temperatures, especially when employed while driving and charging.

Finally, the variation in cell state of health within packs following 10 years of automotive service was studied for 50-kW DCFC. The study employed a multi-cell model only with the active BTMS operated during driving and standby, having recognized its necessity in the previously describe work. Results for maximum thermal gradients show that such gradients regularly

exceed 11 °C in the presence of fast charging. Such gradients, if sustained for long periods of time, would be expected to create large variations in cell state of health within a pack, which would then limit the utility of the vehicle.

The 50-kW DCFC study showed that battery capacity fade will be highly dependent on how often the fast charging stations are used by the consumer as the fade is directly related to the mean temperature of the battery. However, the maximum temperature under certain ambient conditions (Phoenix) and the cell-to-cell temperature variation across the pack were of more concern at the 50-kW level of fast charging. It should also be noted that the power-to-energy ratio of the battery simulated was 6.1, and most 200 + mile BEVs will have a much lower power-to-energy ratio. The cells will therefore be less efficient, and the temperature maximum and variation will be increased. Obviously, each of these parameters will be magnified when utilizing XFC stations on a regular basis. Further studies on cooling strategies will be needed to determine how to keep the batteries below the operational maximum temperature limit during XFC and still be able to provide the driving range desired by consumers.

5. Conclusions

Extreme fast charging will allow the consumer to charge the vehicle battery by 80% in an 8- to 10-min period, which is on par with the refueling time of conventional gasoline-powered vehicles. The ability to charge the BEV this rapidly will decrease the range anxiety of many consumers and will aid in the adoption of BEVs. However, there are many battery thermal considerations that need to be addressed before XFC can become a reality, including:

- A robust BTMS will be required and will be independent of the energy density of the cells; even with high power cells, an oversized BTMS will be needed.
- The size of the BTMS will have to increase from today's BEV average size of 1–5 kW to around 15–25 kW.
- The heat efficiency of high energy density cells will need to improve by 10%–20% at high rates of charge.
- New thermal management strategies like jet impingement or immersion of the battery in a dielectric fluid may need to be investigated to keep the battery below the maximum operational temperature limit.
- The cell-to-cell imbalance due to XFC will affect the longevity and cycle life cost of the cells. New passive and/or active battery management systems will need to be investigated to ensure that the batteries meet the original equipment manufacturer's warranty obligations.
- Cell design will have an impact on the temperature variation within the cell and the temperature imbalance within the pack.
- The mean average temperature of the battery directly affects the cycle life of the battery. High XFC use by the driver will have a strong influence on this metric.
- Additional cooling at the XFC station may be required to ensure a complete charge of the battery pack.

Table 6
Effect of DCFC and BTMSs on battery capacity loss in Seattle and Phoenix [9].

Seattle Climate 10-Year Capacity Loss, %			Phoenix Climate 10-Year Capacity Loss, %		
Strategy	No Fast Charge	Fast Charge	Strategy	No Fast Charge	Fast Charge
Passive Cooling	17.6	18.1	Passive Cooling	27.0	27.6
Active Cooling	17.3	17.5	Active Cooling	24.4	24.5
Active + Standby	17.1	17.3	Active + Standby	21.0	21.2

Table 7
Effect of DCFC and BTMS on maximum battery temperature in Seattle and Phoenix [9].

Seattle Climate Maximum Battery Temperature, °C			Phoenix Climate Maximum Battery Temperature, °C		
Strategy	No Fast Charge	Fast Charge	Strategy	No Fast Charge	Fast Charge
Passive Cooling	32.8	47.2	Passive Cooling	47.8	63.5
Active Cooling	31.2	37.2	Active Cooling	46.3	46.7
Active + Standby	29.6	29.8	Active + Standby	42.5	42.7

XFC from a thermal perspective will be challenging, but it is not an improbable barrier to overcome. Presently, we can address many of the thermal issues by using low energy density or power cells in combination with an oversized BTMS. However, the system will not meet DOE's cost, mass, and volume goals for a BEV, and the cost alone will not allow for large market penetration. To meet DOE's goals, we will need to investigate new thermal management strategies for cell and pack cooling and will need to greatly improve the thermal efficiency of many of the advanced cathodes and anodes presently under development. The cell thermal design for these advanced chemistries will also need to be optimized to limit the life cycle effects on the battery pack associated with XFC.

Acknowledgements

This work was performed under the auspices of the U.S. Department of Energy Office of Vehicle Technologies, under Contract Nos. DE-AC02-06CH11357 (Argonne National Laboratory), DE-DE-AC07-05ID14517 (Idaho National Laboratory), and DE-AC36-08GO28308 (National Renewable Energy Laboratory). The U.S. Government retains for itself, and others acting on its behalf, a paid-up nonexclusive, irrevocable worldwide license in said article to reproduce, prepare derivative works, distribute copies to the public, and perform publicly and display publicly, by or on behalf of the Government.

Acronyms

BEV	battery electric vehicle
BTMS	battery thermal management system
C-Rate	Rate at which a battery is discharged relative to its maximum capacity
DCFC	direct current fast charging

DOE	U.S. Department of Energy
XFC	extreme fast charging (between 150 and 400 kW)
EV	electric vehicle
NMC	nickel, manganese, and cobalt cathode

References

- [1] D. Howell, B. Cunningham, et al., Overview of the DOE VTO Advanced Battery R&D Program, Annual Merit Review, June, 2016.
- [2] V. Srinivasan, C.Y. Wang, Analysis of electrochemical and thermal behavior of Li-ion cells, *J. Electrochem. Soc.* 150 (2003) A98–A106.
- [3] G.-H. Kim, K. Smith, K. Lee, S. Santhanagopalan, A. Pesaran, Multi-domain modeling of lithium-ion batteries encompassing multi-physics in varied length scales, *ECS* 158 (2011) A955–A969.
- [4] Smith, K.; Shi, Ying; Santhanagopalan, Shriram. (2015). Proceedings of the 2015 American Control Conference (ACC), July 1–3, 2015, Chicago, Illinois; pp. 728–730.
- [5] Y.-H. Chen, C.-W. Wang, G. Liu, X.-Y. Song, V.S. Battaglia, A.M. Sastry, Selection of conductive additives in Li-Ion battery cathodes, *ECS* 154 (2007) A978–A986.
- [6] S. Santhanagopalan, K. Smith, J. Neubauer, G.-H. Kim, A. Pesaran, M. Keyser, Design and Analysis of Large Lithium-Ion Battery Systems, Artech House, 2014.
- [7] K. Smith, Y. Shi, E. Wood, A. Pesaran, Optimizing battery usage and management for long life, Advanced Automotive Battery Conference, Detroit, Michigan, June 16, 2016.
- [8] J. Neubauer, E. Wood, E. Burton, K. Smith, A.A. Pesaran, Impact of fast charging on life of EV batteries, EVS28, Kintex, Korea, May 3–6, 2015.
- [9] J.S. Neubauer, E. Wood, Will your battery survive a world with fast chargers? SAE World Congress, Detroit Michigan, April 21–23, 2015.
- [10] K. Smith; Y. Shi; E. Wood, A. Pesaran. Advanced Automotive Battery Conference (AABC), Detroit Michigan, June, 14–17, 2016.
- [11] J. Neubauer, Battery Lifetime Analysis and Simulation Tool (BLAST) Documentation, December, 2014.
- [12] J. Neubauer, E. Wood, Thru-life impacts of driver aggression, climate, cabin thermal management, and battery thermal management on battery electric vehicle utility, *J. Power Sources* 259 (2014) 262–275.
- [13] INL/MIS-13–29877, DC fast Charge Effects on Battery Life and Performance Study – 50,000 Mile Update, April, 2015.